HHS Public Access

Author manuscript

Photochem Photobiol. Author manuscript; available in PMC 2015 August 24.

Published in final edited form as:

Photochem Photobiol. 2012 ; 88(2): 461–468. doi:10.1111/j.1751-1097.2012.01081.x.

Lysosomal Signaling Enhances Mitochondria-Mediated Photodynamic Therapy in A431 Cancer Cells: Role of Iron

Shalini Saggu[1], **Hsin-I Hung**[1], **Geraldine Quiogue**[1], **John J. Lemasters**[1,2,3], and **Anna-Liisa Nieminen**[*,1,3]

[1]Department of Pharmaceutical and Biomedical Sciences, Center for Cell Death, Injury and Regeneration, Medical University of South Carolina, Charleston, SC

[2]Department of Biochemistry and Molecular Biology, Center for Cell Death, Injury and Regeneration, Medical University of South Carolina, Charleston, SC

[3]Hollings Cancer Center, Medical University of South Carolina, Charleston, SC

Abstract

In photodynamic therapy (PDT), light activates a photosensitizer added to a tissue, resulting in singlet oxygen formation and cell death. The photosensitizer phthalocyanine 4 (Pc 4) localizes primarily to mitochondrial membranes in cancer cells, resulting in mitochondria-mediated cell death. The aim of this study was to determine how lysosomes contribute to PDT-induced cell killing by mitochondria-targeted photosensitizers such as Pc 4. We monitored cell killing of A431 cells after Pc 4-PDT in the presence and absence of bafilomycin, an inhibitor of the vacuolar proton pump of lysosomes and endosomes. Bafilomycin was not toxic by itself, but greatly enhanced Pc 4-PDT-induced cell killing. To investigate whether iron loading of lysosomes affects bafilomycin-induced killing, cells were incubated with ammonium ferric citrate (30 μM) for 30 h prior to PDT. Ammonium ferric citrate enhanced Pc 4 plus bafilomycin-induced cell killing without having toxicity by itself. Iron chelators (desferrioxamine and starch-desferrioxamine) and the inhibitor of the mitochondrial calcium (and ferrous iron) uniporter, Ru360, protected against Pc 4 plus bafilomycin toxicity. These results support the conclusion that chelatable iron stored in the lysosomes enhances the efficacy of bafilomycin-mediated PDT and that lysosomal disruption augments PDT with Pc 4.

INTRODUCTION

Photodynamic therapy (PDT) involves administration of a photosensitizing drug followed by photoirradiation with light absorbed by the photosensitizer. PDT to target cells and tissues results in generation of singlet oxygen ($^1O_2$) and/or other reactive oxygen species (ROS) that oxidize tissue lipids and proteins, resulting in oxidative stress and cell death. Besides the intensity of light and concentration of photosensitizer, the subcellular localization of a photosensitizer is also critical to determining the efficacy of the PDT treatment (reviewed in [1]). Photosensitizers usually target three main organelles: mitochondria, endoplasmic reticulum and lysosomes (1–5). PDT mediated by a

*Corresponding author nieminen@musc.edu (Anna-Liisa Nieminen).

mitochondria-targeted photosensitizer directly dissipates the mitochondrial membrane potential (2) whereas, alternatively, PDT with a lysosome-targeted photosensitizer causes a release of lysosomal constituents (5). Due to release of lysosomal constituents, lysosome-targeted photosensitizers seem to be more efficient in cell killing than ones targeted to mitochondria. Indeed, our previous studies have shown that analogs of Pc 4 that primarily localize to lysosomes are more effective in killing after PDT (6,7).

For our previous studies, we used Pc 4 as a photosensitizer. Pc 4 is a silicon phthalocyanine bearing a dimethylaminopropylsiloxy ligand on the central silicon (8). Pc 4 localizes primarily to mitochondria, endoplasmic reticulum and to a lesser extent lysosomes, as assessed by confocal microscopy (2,3). Pc 4-PDT induces apoptotic cell death that is mediated by formation of mitochondrial ROS leading to onset of the mitochondrial permeability transition, mitochondrial swelling and cytochrome *c* release (2).

In this study, our aim was to determine how lysosomes contribute to PDT induced by mitochondria-targeted photosensitizers such as Pc 4. Specifically, we focused on the role of lysosomal iron in PDT killing. In cells and tissues, two pools of iron exist. The first pool is "nonchelatable" iron that is sequestered in ferritin and structural components of proteins (*e.g.* heme, iron-sulfur complexes), which cannot be removed by iron chelators like desferrioxamine (DFO). The second pool is "chelatable" iron, which represents free iron and iron bound loosely to a wide variety of anionic intracellular molecules (9). Chelatable iron is accessible to DFO and other iron chelators. Chelatable iron and other transition metals such as copper catalyze formation of highly reactive hydroxyl radical ($OH^{\bullet}$) from H_2O_2 and superoxide ($O_2^{\bullet -}$). $OH^{\bullet}$ damages DNA, proteins and membranes (10). The toxicity of iron is manifested by onset of the mitochondrial permeability transition (MPT) and consequent necrotic and apoptotic cell death of hepatocytes after exposure to a membrane permeable Fe^{3+} complex (11).

Lysosomes are a source of rapidly mobilized chelatable iron that when released into the cytosol is rapidly taken up by mitochondria through the calcium uniporter (12–15). Inside mitochondria, this iron is available to catalyze toxic ROS cascades. Therefore, we hypothesized that iron translocation from lysosomes to mitochondria would enhance PDT-induced cell killing with mitochondria-targeted photosensitizers. Our results demonstrate that exogenous iron together with inhibition of the vacuolar proton-pumping ATPase greatly enhances mitochondria-targeted Pc 4-PDT-mediated apoptotic death.

MATERIALS AND METHODS

Cell culture

Human A431 epidermoid carcinoma cells were obtained from American Type Culture Collection. Cells were cultured in Dulbecco's Modified Eagle's Medium (DMEM) supplemented with 10% fetal bovine serum (FBS) and penicillin/streptomycin (complete culture medium) in humidified 5% CO_2/95% air at 37°C.

PDT

The phthalocyanine photosensitizer Pc 4 was obtained from Dr. Malcolm Kenney (Case Western Reserve University; 6). A stock solution of 0.5 mM was made in dimethyl formamide and diluted into complete culture medium. Cell cultures were incubated with 25 or 50 nM Pc 4, as indicated, for 16–18 h before exposure to red light (λ = 670 nm, 350 mJ cm^{-2}, 1.1 mW cm^{-2}) at 37°C from an Intense-HPD 7404 diode laser (North Brunswick, NJ). Subsequently, cells were returned to the incubator prior to assays at designated times.

Clonogenic assay

Cells (330 000 per dish) were cultured in 60-mm Petri dishes for 24 h. Subsequently, cells were loaded with 25 nM Pc 4 for 16–18 h. One hour prior to irradiation, 50 nM bafilomycin was added, as indicated. Immediately after irradiation, cells were harvested by trypsinization. Aliquots of cell suspensions were plated onto 60-mm Petri dishes in amounts sufficient to yield 50–100 colonies per dish. After 14 days in complete culture medium, colonies were stained with 0.1% crystal violet in 20% ethanol and counted by eye.

Caspase 3/7 activity

Caspase-3/7 activity was measured using a Caspase-Glo™ 3/7 kit (Promega, Madison, WI) according to the manufacturer's instructions. At indicated time points, cultured cells were scraped into a test tube followed by centrifugation. The pellet was resuspended and lysed with RIPA (150 mM NaCl, 1 mM EGTA, 1% sodium deoxycholate, 1% Triton X-100, 50 mM Tris-Cl, pH 7.4) buffer. Caspase-Glo™ 3/7 reagent and the lysate were mixed in 1:1 ratio, and luminescence was measured with a luminometer. The resulting luminescence was proportional to caspase activity.

Assessment of cell death

Cell death was assessed by propidium iodide (PI) fluorometry using a multiwell fluorescence plate reader, as previously described (16). Briefly, cells were cultured on 96-well plates (6 000 cells per well) for 48 h in complete culture medium. Pc 4 (25 nM), DFO (1 mM) and starch-DFO (sDFO; 1 mM) were present during the last 18 h of the incubation. Subsequently, medium was aspirated and changed to fresh medium supplemented with Insulin-Transferrin-Selenium-X reagent (Gibco; insulin [10 μg mL^{-1}], transferrin [5.5 μg mL^{-1}], selenium [6.7 ng mL^{-1}], ethanolamine [0.2 mg mL^{-1}]), and containing PI (30 μM), but omitting FBS. Bafilomycin (50 nM) and chloroquine (50 μM) were added as indicated. One hour after drug addition but before irradiation, PI fluorescence was measured using 530-nm excitation (25-nm band pass) and 620-nm emission (40-nm band pass) filters. PI fluorescence was then measured at frequent intervals for 12 h. Between measurements, microtiter plates were placed in a 37°C incubator. At the end of the experiment, digitonin (200 μM) was added to each well to permeabilize all cells and label all nuclei with PI. Fluorescence was measured again to obtain a value corresponding to 100% cell death. Percentage viability (V) was calculated as $V = 100(X - A)/(B - A)$, where A is initial fluorescence, B is fluorescence after addition of digitonin, and X is fluorescence after any given time. Cell viability determined by PI fluorometry is essentially the same as cell viability determined by trypan blue exclusion (16).

Apoptosis was determined from nuclear morphology after PI staining in the presence of digitonin. At indicated time points, floating and adherent cells were collected, centrifuged and resuspended in PBS containing 100 μM digitonin and 30 μM PI. Digitonin permeabilizes the plasma membrane and allows PI to enter cells and stain all nuclei. Thus, PI staining in the presence of digitonin is equivalent to staining with Hoechst and DAPI, the two fluorescent dyes most commonly used to assess apoptosis by nuclear morphology. Apoptotic nuclei were scored as apoptotic based on nuclear condensation and fragmentation and counted with a 40× microscope objective using a rhodamine filter set and expressed as a percentage of total cells. At least 200 cells were counted from three different microscopic fields for each sample.

Mitochondrial membrane potential

Cells were cultured on 35-mm glass-bottomed Petri dishes (MatTek Corporation, Ashland, MA) at 150 000 cells per dish and loaded with 150 nM tetramethylrhodamine methyl ester (TMRM) for 30 min in culture medium. Dishes were placed in an environmental chamber at 37°C on the stage of Zeiss LSM 510 laser scanning confocal microscope (Zeiss, Germany). A 63 X N.A. 1.4 oil immersion planapochromat objective was used for all experiments. After collecting baseline images of red TMRM fluorescence, cells were exposed to light (350 mJ cm^{-2}), and images were subsequently collected over time using confocal microscopy (543 nm excitation, 560 nm long-pass emission). Cells in images were outlined using Adobe Photoshop (Version CS4) software (Mountain View, CA). Average TMRM fluorescence intensity of the outlined cells was then quantified followed by background subtraction to yield cell specific mean TMRM fluorescence intensity.

Lysosomal integrity

To assess the lysosomal integrity, cells were incubated with 0.2 mg mL^{-1} of Alexa-488 dextran (10 kDa) for 18 h. Alexa-488 dextran is taken up by cells *via* endocytosis. Alexa-488 fluorescence was imaged by confocal microscopy (488 nm excitation/500–530 nm emission). Bright green dots colocalized with lysosome-specific fluorophores (data not shown), such as LysoTracker Red, indicating that Alexa-488 dextran can be used as an endosomal/lysosomal marker.

To assess LysoTracker Red release from lysosomes, cells were incubated with LysoTracker Red (500 nM) for 20 min at 37°C in complete culture medium. Medium was replaced with fresh medium supplemented with 200 nM LysoTracker. LysoTracker Red fluorescence was imaged by confocal microscopy (543 nm excitation/560 nm long-pass emission).

Western blot analysis

Total cell extracts were prepared in ice-cold RIPA lysis buffer supplemented with a cocktail of protease inhibitors (Roche Diagnostics, Indianapolis, IN). The lysates were centrifuged, and the resulting supernatants were assayed for total protein content (Bio-Rad, Hercules, CA). Equivalent amounts of protein were diluted in sample buffer (200 mM Tris-Cl, 15% glycerol, 10% SDS, 5% β-mercaptoethanol, 0.01% bromophenol blue, pH 6.8) and resolved on 12% SDS-PAGE. Proteins were then transferred and immobilized on PVDF membranes (Millipore, Bedford, MA) and probed with anti-HIF-1α (1:1 000, a gift from Dr. Faton

Agani, Case Western Reserve University) and antiactin (1:3 000, Sigma). Immunodetection was accomplished by an enhanced chemiluminescence detection system (Pierce, Rocklord, IL).

Statistical analysis

Data are presented as means ± SEM with n as the number (three or more) of independent experiments. Differences were assessed by Student's *t*-test with INSTAT Software (GraphPAD, San Diego, CA). One-tailed tests were used to test unidirectional hypotheses. A *P*-value < 0.05 was considered to be statistically significant.

RESULTS

Bafilomycin enhances Pc 4-PDT-induced cell killing

Lysosomes are a primary source for "chelatable iron," which is free iron and iron bound loosely to a wide variety of anionic intracellular molecules (9). Chelatable Fe^{2+} reacts with H_2O_2 to generate the highly reactive and toxic hydroxyl radical ($OH^{\bullet}$). The importance of iron-catalyzed $OH^{\bullet}$ formation in cell killing is underscored by the fact that the iron chelator, DFO, suppresses ROS generation and prevents the mitochondrial permeability transition and cell death after oxidative stress to hepatocytes (17). Bafilomycin is an inhibitor of the vacuolar proton-pumping ATPase (18). Consequently, bafilomycin collapses acidic lysosomal/endosomal pH gradients, which leads to release of lysosomal iron into the cytosol (12). To determine if bafilomycin sensitizes Pc 4-PDT-mediated cell killing, A431 epidermoid carcinoma cells were loaded with 25 nM Pc 4 for 18 h followed by 1 h incubation with 50 nM bafilomycin. Subsequently, cells were exposed to light (350 mJ cm^{-2}) at 37°C. For these experiments, we chose a concentration of Pc 4 that by itself did not induce cell killing after irradiation during the course of the experiment. Pc 4-PDT and bafilomycin alone caused no cell killing as evaluated using PI fluorometry (Fig. 1a). By contrast, the combination of Pc 4-PDT plus bafilomycin caused substantial cytotoxicity. Cell viability was 92.8 and 47.2% 12 h after Pc 4-PDT and Pc 4-PDT plus bafilomycin, respectively (Fig. 1a). The results were confirmed with a clonogenic assay (Fig. 1b). In initial experiments, we performed dose-reponse studies with increasing concentrations of Pc 4 in the presence and absence of bafilomycin. At greater Pc 4 concentrations (50–300 nM), a similar enhancement of cell killing by bafilomycin occurred, except that overall cell killing was more rapid, and the killing curves shifted to the left (data not shown).

The PI fluorometry assay monitors failure of the plasma membrane permeability barrier, an event that occurs during necrosis and late stage apoptosis, the latter often named secondary necrosis. To determine further the mode of cell death, apoptosis and caspase 3/7 activity were monitored. Both caspase-3/7 activity and apoptotic death were enhanced by bafilomycin after Pc 4-PDT treatment. Moreover, the pan caspase inhibitor z-VAD completely blocked Pc 4 plus bafilomycin-induced caspase activation and apoptosis (Fig. 1c,d). Overall, the results indicate that bafilomycin enhances mitochondria-targeted Pc 4-PDT toxicity, but alone is nontoxic.

Chloroquine enhances Pc 4-PDT-induced cell killing

To determine whether another agent that causes lysosomal alkalinization has the same effect as bafilomycin, we pretreated cells with chloroquine. Chloroquine is a weak base that accumulates into acidic vesicles and raises their pH (19). Chloroquine alone did not induce cell killing, but combined with Pc 4-PDT enhanced toxicity similar to bafilomycin (Fig. 2a). These results indicate that enhanced killing with bafilomycin and chloroquine after Pc 4-PDT is initiated through a lysosomal/endosomal pathway.

Lysosomal iron augments Pc 4 plus bafilomycin-PDT-mediated cell killing

The results of Fig. 1 show that bafilomycin enhances cell killing by PDT with a mitochondria-targeted photosensitizer. To assess whether iron participates in cell killing after Pc 4-PDT, we preincubated cells with 30 μ_M ammonium iron (III) citrate (Fe^{3+}) for 24 h before Pc 4 loading. Fe^{3+} binds to transferrin, which is taken up by cells through receptor-mediated endocytosis, resulting in increased lysosomal iron. After Fe^{3+} loading, cells were loaded with Pc 4 followed by bafilomycin or vehicle and light irradiation. At the low concentration of Pc 4 used, PDT in the absence and presence of Fe^{3+} caused virtually no toxicity (Fig. 2b). By contrast, in the presence of bafilomycin, Fe^{3+} nearly doubled the rate of Pc 4-PDT-induced killing, decreasing viability to 25% at 12 h after PDT from 47% in the absence of bafilomycin.

Bafilomycin enhances PDT toxicity through mitochondrial depolarization

To determine the role of mitochondrial depolarization in bafilomycin-enhanced cell killing after PDT, we monitored mitochondrial membrane potential from uptake of TMRM visualized by confocal microscopy. Bafilomycin (50 n_M) and Pc 4-PDT alone caused no decrease of TMRM fluorescence (data not shown). After 45 min of Pc 4-PDT plus bafilomycin, a small portion of mitochondria depolarized (Fig. 3a,b). Subsequently, mitochondria further depolarized (Fig. 3b). Preincubation with Fe^{3+} followed by bafilomycin accelerated mitochondrial dysfunction and subsequent cell killing after Pc 4-PDT with depolarization of approximately half the mitochondria after 45 min and nearly all mitochondria after 120 min (Fig. 3a,b). These results show that iron augments mitochondrial dysfunction after Pc 4-PDT.

Protection against mitochondrial depolarization by iron chelators

As previous study indicates that bafilomycin releases free iron from the lysosomes (12), we characterized the effect of iron chelators on mitochondrial depolarization during PDT. Cells were pretreated with DFO (1 m_M) for 18 h before bafilomycin and subsequent irradiation. In the presence of DFO, mitochondrial depolarization after Pc 4-PDT plus bafilomycin following pretreatment with Fe^{3+} was subtantially decreased (Fig. 3a, Pc 4 + Baf + DFO). After 2 h, 57% of TMRM fluorescence was still remaining in the presence of DFO compared with 8% in the absence of DFO (Fig. 3b). Moreover, DFO increased cell viability from 25% to 75% after 12 h (Fig. 3c). sDFO (1 m_M), which is taken up by endocytosis like Alexa-488 dextran and specifically chelates endosomal/lysosomal iron, blocked mitochondrial depolarization after Pc 4-PDT to an even greater extent than DFO (Fig. 3a, Pc 4 + Baf + sDFO; Fig. 3b). sDFO also increased viability from 25% to 63% after 12 h (Fig.

3c). To confirm that iron chelators simply did not reverse the effect of added iron, we assessed the effect of DFO and sDFO on viability during Pc 4-PDT (50 nM Pc 4) plus bafilomycin in the absence of Fe^{3+}. Both DFO and sDFO protected against Pc 4-PDT plus bafilomycin (Fig. 3d).

To determine whether bafilomycin-enhanced mitochondrial dysfunction after PDT was dependent on lysosomal membrane breakdown, cells were preloaded with Fe^{3+}, Alexa-488 dextran (10 kDa), and Pc 4 (25 nM). Alexa-488 dextran is taken up by endocytosis to label endosomes/lysosomes as bright fluorescent dots (Fig. 4a, Pc 4 + Fe). Subsequent 1 h exposure of bafilomycin did not change endosomal/lysosomal integrity (Fig. 4a; + Baf). After 2 h of irradiation, although mitochondrial depolarization was maximal there was no change in Alexa-488 dextran fluorescence (Fig. 4a, + Baf + Light; cf. Fig. 3b). To confirm that bafilomycin collapsed lysosomal pH gradient, cells were loaded with LysoTracker Red (500 nM) and subsequently exposed to bafilomycin. LysoTracker Red is a weak base and accumulates into acidic organelles such as lysosomes (20). Inhibition of the vacuolar proton-pumping ATPase with bafilomycin is well established to collapse lysosomal pH gradients and induce lysosomal alkalinization. Release of LysoTracker Red after bafilomycin in our experiments serves to confirm that bafilomycin was penetrating the cells and acting as expected (Fig. 4b). We also loaded lysosomes with Alexa-488 dextran (10 kDa). After 1 h exposure to bafilomycin, lysosomes retained Alexa-488 dextran, but released LysoTracker Red (compare Fig. 4a with b), which shows lysosomal alkalinization without generalized lysosomal membrane permeabilization. In addition, imaging of Alexa-488 dextran did not show evidence of lysosomal swelling after bafilomycin, which would be expected as a colloid osmotic effect if the membrane became nonspecifically permeable to smaller molecular weight solutes. Indeed, nonspecific permeabilization to small or large molecular weight solutes has never been described for bafilomycin. Rather bafilomycin is a very specific and high-affinity inhibitor of the lysosomal proton pump (18).

Bright LysoTracker Red-labeled spots disappeared after bafilomycin, indicating lysosomal alkalinization (Fig. 4b). These results indicate that bafilomycin-enhanced mitochondrial dysfunction was not due to endosomal/lysosomal membrane breakdown, but rather through collapse of the pH gradient in these organelles, which promotes release into the cytosol of lysosomal chelatable iron.

Protection against mitochondrial depolarization by Ru360

Ru360 is a highly specific inhibitor of the mitochondrial electrogenic calcium uniporter (21). When cytosolic ferrous iron increases, the calcium uniporter translocates the iron into mitochondria (12,14). Ru360 (10 μM) blocked bafilomycin-induced mitochondrial depolarization after Pc 4-PDT following Fe^{3+} (Fig. 5a, Pc 4 + Baf + Ru360; Fig. 5b). Ru360 also increased viability from 25% to 57% (Fig. 5c).

Iron chelators, such as DFO, stabilize hypoxia-inducible factor 1 alpha (HIF-1α) by inhibiting proline hydroxylase, an enzyme that promotes HIF-1α proteasomal degradation (22). As HIF-1α target genes are protective, DFO-mediated protection against PDT may not be due to chelation of iron *per se*, but rather to increased HIF-1α levels. Accordingly, we assessed HIF-1α protein by Western immunoblotting 18 h after incubation of cells with

DFO, sDFO and Ru360 without pretreatment with Fe^{3+}. As expected, DFO and sDFO increased HIF-1α protein levels compared with untreated cells. However, Ru360 did not increase HIF-1α, although Ru360 did block mitochondrial depolarization and cell death after Pc 4-PDT plus bafilomycin (Fig. 6). Therefore, Ru360-mediated protection cannot be explained by upregulation of HIF-1α.

DISCUSSION

Our results show that bafilomycin greatly accelerates mitochondrion-specific Pc 4-PDT-mediated cell killing. Although bafilomycin acts on lysosomes, its toxic effects were manifested in mitochondria by accelerated depolarization after PDT, resulting in caspase 3/7 activation and apoptotic death. The findings indicate a cross-talk between lysosomes and mitochondria during PDT.

The endodomal/lysosomal compartment continuously receives iron by transferrin receptor-mediated endocytosis and autophagic digestion of iron-containing proteins (23,24). Thus, lysosomes are a reservoir of chelatable, redox-active Fe^{2+}. Fe^{2+} reacts with H_2O_2 to generate highly reactive and toxic $OH^{\bullet}$. The importance of iron-catalyzed ROS formation in cell killing is underscored by the fact that DFO suppresses ROS generation and prevents the mitochondrial permeability transition and cell death after oxidative stress to hepatocytes (12,17). During Pc 4-PDT, a large proportion of ROS formation occurs inside mitochondria and leads to onset of the mitochondrial permeability transition, as documented by increased mitochondrial dichlorofluorescein fluorescence and movement of calcein across the mitochondrial inner membrane (2).

Alkalinization of lysosomes/endosomes with bafilomycin enhanced Pc 4-PDT-mediated cell killing (Fig. 1). However, bafilomycin did not induce lysosomal membrane breakdown after Pc 4-PDT, as assessed by retention of 10 kDa Alexa-488 dextran with lysosomes (Fig. 3b). Alexa-488 dextran fluorescence is pH-independent and therefore loss of Alexa-488 dextran fluorescence signifies specifically lysosomal disintegration rather than a change in lysosomal pH. Other lysomotropic fluorophores (*e.g.* acridine orange, LysoTracker Red and LysoTracker Green) have been widely used to assess lysosomal damage after oxidative stress. These probes are weak bases that accumulate into acidic organelles, mainly lysosomes. Release of these probes from lysosomes after oxidative stress is often interpreted as lysosomal membrane damage and disintegration (25,26). However, after bafilomycin and chloroquine, lysosomes released LysoTracker Red without loss of Alexa-488 dextran fluorescence, signifying that lysosomal membranes remained intact (Fig. 4b).

Fe^{3+} forms a complex with transferrin, which binds to transferrin receptors for receptor-mediated endocytosis, resulting in iron delivery to endosomes/lysosomes. The observation that preincubation of cells with Fe^{3+} enhanced killing after bafilomycin plus Pc 4-PDT treatment and that sDFO prevented this cell killing is consistent with the conclusion that bafilomycin mobilizes iron from lysosomes into the cytosol. Similar results were obtained in a recent study with HeLa cells, where $FeCl_3$ enhanced ionizing radiation-induced killing that was prevented by iron chelation (27).

Fe^{2+} reacts with H_2O_2 to form $OH^{\bullet}$, a highly reactive form of ROS (28). Bafilomycin by itself was not sufficient to induce mitochondrial depolarization (data not shown) or cell killing (Fig. 1a). Rather, mild oxidative stress induced by low dose Pc 4-PDT combined with bafilomycin was needed to induce mitochondrial depolarization (Fig. 3a,b). The iron chelators, DFO and sDFO, protected against PDT plus bafilomycin-induced mitochondrial depolarization and killing (Fig. 3). DFO is highly polar and poorly permeant through membranes, and therefore millimolar concentrations were required to protect. DFO may also be taken up by endocytosis resulting in its accumulation in endosomes/lysosomes (29). Consequently, cytoprotection with DFO may be explained by chelation of redox-active iron in lysosomes. sDFO also prevented PDT plus bafilomycin-induced mitochondrial depolarization and cell killing (Fig. 3), indicating that lysosomes/endosomes release redox-active iron after bafilomycin and that DFO and sDFO prevent this release by chelating the intraluminal iron store of these organelles.

Protection by lysosomal iron chelation against mitochondrial depolarization after PDT suggests that mitochondrial iron uptake may be responsible for bafilomycin-enhanced killing. Mitochondria accumulate Fe^{2+}, but not Fe^{3+}, electrogenically *via* the mitochondrial Ca^{2+} uniporter (14). The highly specific inhibitor of calcium uniporter, Ru360, also protected against bafilomycin-enhanced mitochondrial depolarization during PDT (Fig. 5a,b). Although Ru360 and iron chelators completely blocked mitochondrial depolarization, iron chelators were somewhat more effective in protecting against cell killing (Figs. 3 and 5). Thus, chelation of extra-mitochondrial redox-active iron may also contribute to cytoprotection by iron chelators.

In Jurkat cells exposed to H_2O_2, iron binding to a thiol group in the active center of procaspase 9 inactivated the enzyme and blocked the progression of apoptosis (30). Such an event did not seem to be occurring in our study, as both iron chelators and Ru360 inhibited mitochondrial depolarization, which is upstream of caspase 9 activation. Another effect of iron chelators is to stabilize HIF-1α in normoxic cells (22,31). HIF-1α activates several protective signaling pathways that potentially could explain cytoprotection by iron chelation. Although DFO and sDFO did stabilize HIF-1α protein levels, Ru360 did not (Fig. 6). As Ru360 protected against mitochondrial depolarization similarly to DFO/sDFO, HIF-1α is not likely responsible for cytoprotection.

Bafilomycin is frequently used to inhibit autophagy by collapsing lysosomal pH gradient and thereby blocking fusion of autophagosomes with lysosomes (32). Consistently with an effect on autophagy, bafilomycin alone and Pc 4-PDT plus bafilomycin increased cellular LC-3 II protein levels as assessed by Western blotting presumably by inhibiting fusion of autophagosomes with lysosomes (data not shown). Thus, bafilomycin was inhibiting autophagic flux, which might be a reason for increased PDT killing with bafilomycin. However, iron chelators and Ru360 protected cells against Pc 4-PDT plus bafilomycin toxicity, but neither iron chelators nor Ru360 altered LC-3 II protein levels (data not shown). Thus, it seems unlikely that enhanced survival by iron chelators and Ru360 acts through enhancing autophagy. Rather, iron chelators and Ru360 prevented mitochondrial depolarization induced by bafilomycin during PDT (Figs. 3 and 5).

In conclusion, we established a link between lysosomal alkalinization and mitochondrial depolarization during PDT (Fig. 7). Strategies to engage lysosomes in cell death pathways have potential to enhance tumor cell killing. Herein, our results demonstrate that strategies to collapse the lysosomal pH gradient without lysosomal membrane breakdown is sufficient to induce iron-dependent mitochondrial depolarization and subsequent cell killing. Lysosomal perturbation by bafilomycin effectively enhances mitochondria-mediated cell killing during PDT. Pc 4-PDT has completed a Phase I clinical trial for cutaneous neoplasms (33) and is currently in a Phase I trial for psoriasis. The results of this study suggest that agents that disturb lysosomal function could potentially be used clinically as an adjuvant treatment with mitochondria-targeted photosensitizers.

Acknowlegements

This research was supported by grants from the US National Cancer Institute, R01 CA119079, P30 CA138313 (Hollings Cancer Center Cell and Molecular Imaging Shared Resource) and Abney Foundation Fellowship to Hsin-I Hung.

REFERENCES

1. Oleinick NL, Morris RL, Belichenko I. The role of apoptosis in response to photodynamic therapy: what, where, why, and how. Photochem. Photobiol. Sci. 2002; 1:1–21. [PubMed: 12659143]
2. Lam M, Oleinick NL, Nieminen AL. Photodynamic therapy-induced apoptosis in epidermoid carcinoma cells. Reactive oxygen species and mitochondrial inner membrane permeabilization. J. Biol. Chem. 2001; 276:47379–47386. [PubMed: 11579101]
3. Trivedi NS, Wang HW, Nieminen AL, Oleinick NL, Izatt JA. Quantitative analysis of Pc 4 localization in mouse lymphoma (LY-R) cells *via* double-label confocal fluorescence microscopy. Photochem. Photobiol. 2000; 71:634–639. [PubMed: 10818795]
4. Kessel D, Price M, Caruso J, Reiners J Jr. Effects of photodynamic therapy on the endocytic pathway. Photochem. Photobiol. Sci. 2011; 10:491–498. [PubMed: 21125114]
5. Reiners JJ Jr. Caruso JA, Mathieu P, Chelladurai B, Yin XM, Kessel D. Release of cytochrome *c* and activation of pro-caspase-9 following lysosomal photodamage involves bid cleavage. Cell Death Differ. 2002; 9:934–944. [PubMed: 12181744]
6. Rodriguez ME, Zhang P, Azizuddin K, Delos Santos GB, Chiu SM, Xue LY, Berlin JC, Peng X, Wu H, Lam M, Nieminen AL, Kenney ME, Oleinick NL. Structural factors and mechanisms underlying the improved photodynamic cell killing with silicon phthalocyanine photosensitizers directed to lysosomes *versus* mitochondria. Photochem. Photobiol. 2009; 85:1189–1200. [PubMed: 19508642]
7. Chiu SM, Xue LY, Lam M, Rodriguez ME, Zhang P, Kenney ME, Nieminen AL, Oleinick NL. A requirement for bid for induction of apoptosis by photodynamic therapy with a lysosome—but not a mitochondrion-targeted photosensitizer. Photochem. Photobiol. 2010; 86:1161–1173. [PubMed: 20553412]
8. Oleinick NL, Antunez AR, Clay ME, Rihter BD, Kenney ME. New phthalocyanine photosensitizers for photodynamic therapy. Photochem. Photobiol. 1993; 57:242–247. [PubMed: 8451285]
9. Ma Y, De GH, Liu Z, Hider RC, Petrat F. Chelation and determination of labile iron in primary hepatocytes by pyridinone fluorescent probes. Biochem. J. 2006; 395:49–55. [PubMed: 16336208]
10. Kehrer JP. The Haber-Weiss reaction and mechanisms of toxicity. Toxicology. 2000; 149:43–50. [PubMed: 10963860]
11. Rauen U, Petrat F, Sustmann R, de Groot H. Iron-induced mitochondrial permeability transition in cultured hepatocytes. J. Hepatol. 2004; 40:607–615. [PubMed: 15030976]
12. Uchiyama A, Kim JS, Kon K, Jaeschke H, Ikejima K, Watanabe S, Lemasters JJ. Translocation of iron from lysosomes into mitochondria is a key event during oxidative stress-induced hepatocellular injury. Hepatology. 2008; 48:1644–1654. [PubMed: 18846543]

13. De SD, Raffaello A, Teardo E, Szabo I, Rizzuto R. A forty-kilodalton protein of the inner membrane is the mitochondrial calcium uniporter. Nature. 2011; 476:336–340. [PubMed: 21685888]
14. Flatmark T, Romslo I. Energy-dependent accumulation of iron by isolated rat liver mitochondria. Requirement of reducing equivalents and evidence for a unidirectional flux of Fe(II) across the inner membrane. J. Biol. Chem. 1975; 250:6433–6438. [PubMed: 808543]
15. Baughman JM, Perocchi F, Girgis HS, Plovanich M, Belcher-Timme CA, Sancak Y, Bao XR, Strittmatter L, Goldberger O, Bogorad RL, Koteliansky V, Mootha VK. Integrative genomics identifies MCU as an essential component of the mitochondrial calcium uniporter. Nature. 2011; 476:341–345. [PubMed: 21685886]
16. Nieminen AL, Gores GJ, Bond JM, Imberti R, Herman B, Lemasters JJ. A novel cytotoxicity screening assay using a multiwell fluorescence scanner. Toxicol. Appl. Pharmacol. 1992; 115:147–155. [PubMed: 1641848]
17. Byrne AM, Lemasters JJ, Nieminen AL. Contribution of increased mitochondrial free Ca^{2+} to the mitochondrial permeability transition induced by tert-butylhydroperoxide in rat hepatocytes. Hepatology. 1999; 29:1523–1531. [PubMed: 10216138]
18. Gagliardi S, Rees M, Farina C. Chemistry and structure activity relationships of bafilomycin A1, a potent and selective inhibitor of the vacuolar H^+-ATPase. Curr. Med. Chem. 1999; 6:1197–1212. [PubMed: 10519916]
19. Poole B, Ohkuma S. Effect of weak bases on the intralysosomal pH in mouse peritoneal macrophages. J. Cell Biol. 1981; 90:665–669. [PubMed: 6169733]
20. Griffiths G, Hoflack B, Simons K, Mellman I, Kornfeld S. The mannose 6-phosphate receptor and the biogenesis of lysosomes. Cell. 1988; 52:329–341. [PubMed: 2964276]
21. Ying WL, Emerson J, Clarke MJ, Sanadi DR. Inhibition of mitochondrial calcium ion transport by an oxo-bridged dinuclear ruthenium ammine complex. Biochemistry. 1991; 30:4949–4952. [PubMed: 2036363]
22. Knowles HJ, Raval RR, Harris AL, Ratcliffe PJ. Effect of ascorbate on the activity of hypoxia-inducible factor in cancer cells. Cancer Res. 2003; 63:1764–1768. [PubMed: 12702559]
23. Klausner RD, Ashwell G, van Renswoude J, Harford JB, Bridges KR. Binding of apotransferrin to K562 cells: explanation of the transferrin cycle. Proc. Natl Acad. Sci. USA. 1983; 80:2263–2266. [PubMed: 6300904]
24. Iacopetta BJ, Morgan EH. The kinetics of transferrin endocytosis and iron uptake from transferrin in rabbit reticulocytes. J. Biol. Chem. 1983; 258:9108–9115. [PubMed: 6135697]
25. Tenopoulou M, Doulias PT, Barbouti A, Brunk U, Galaris D. Role of compartmentalized redox-active iron in hydrogen peroxide-induced DNA damage and apoptosis. Biochem. J. 2005; 387:703–710. [PubMed: 15579135]
26. Lin Y, Epstein DL, Liton PB. Intralysosomal iron induces lysosomal membrane permeabilization and cathepsin D-mediated cell death in trabecular meshwork cells exposed to oxidative stress. Invest. Ophthalmol. Vis. Sci. 2010; 51:6483–6495. [PubMed: 20574010]
27. Berndt C, Kurz T, Selenius M, Fernandes AP, Edgren MR, Brunk UT. Chelation of lysosomal iron protects against ionizing radiation. Biochem. J. 2010; 432:295–301. [PubMed: 20846118]
28. Halliwell B. The wanderings of a free radical. Free Radic. Biol. Med. 2009; 46:531–542. [PubMed: 19111608]
29. Cable H, Lloyd JB. Cellular uptake and release of two contrasting iron chelators. J. Pharm. Pharmacol. 1999; 51:131–134. [PubMed: 10217310]
30. Barbouti A, Amorgianiotis C, Kolettas E, Kanavaros P, Galaris D. Hydrogen peroxide inhibits caspase-dependent apoptosis by inactivating procaspase-9 in an iron-dependent manner. Free Radic. Biol. Med. 2007; 43:1377–1387. [PubMed: 17936184]
31. Jaakkola P, Mole DR, Tian YM, Wilson MI, Gielbert J, Gaskell SJ, Kriegsheim A, Hebestreit HF, Mukherji M, Schofield CJ, Maxwell PH, Pugh CW, Ratcliffe PJ. Targeting of HIF-alpha to the von Hippel-Lindau ubiquitylation complex by O_2-regulated prolyl hydroxylation. Science. 2001; 292:468–472. [PubMed: 11292861]
32. Yamamoto A, Tagawa Y, Yoshimori T, Moriyama Y, Masaki R, Tashiro Y. Bafilomycin A1 prevents maturation of autophagic vacuoles by inhibiting fusion between autophagosomes and

lysosomes in rat hepatoma cell line, H-4-II-E cells. Cell Struct. Funct. 1998; 23:33–42. [PubMed: 9639028]

33. Baron ED, Malbasa CL, Santo-Domingo D, Fu P, Miller JD, Hanneman KK, Hsia AH, Oleinick NL, Colussi VC, Cooper KD. Silicon phthalocyanine (Pc 4) photodynamic therapy is a safe modality for cutaneous neoplasms: results of a phase 1 clinical trial. Lasers Surg. Med. 2010; 42:728–735. [PubMed: 21246576]

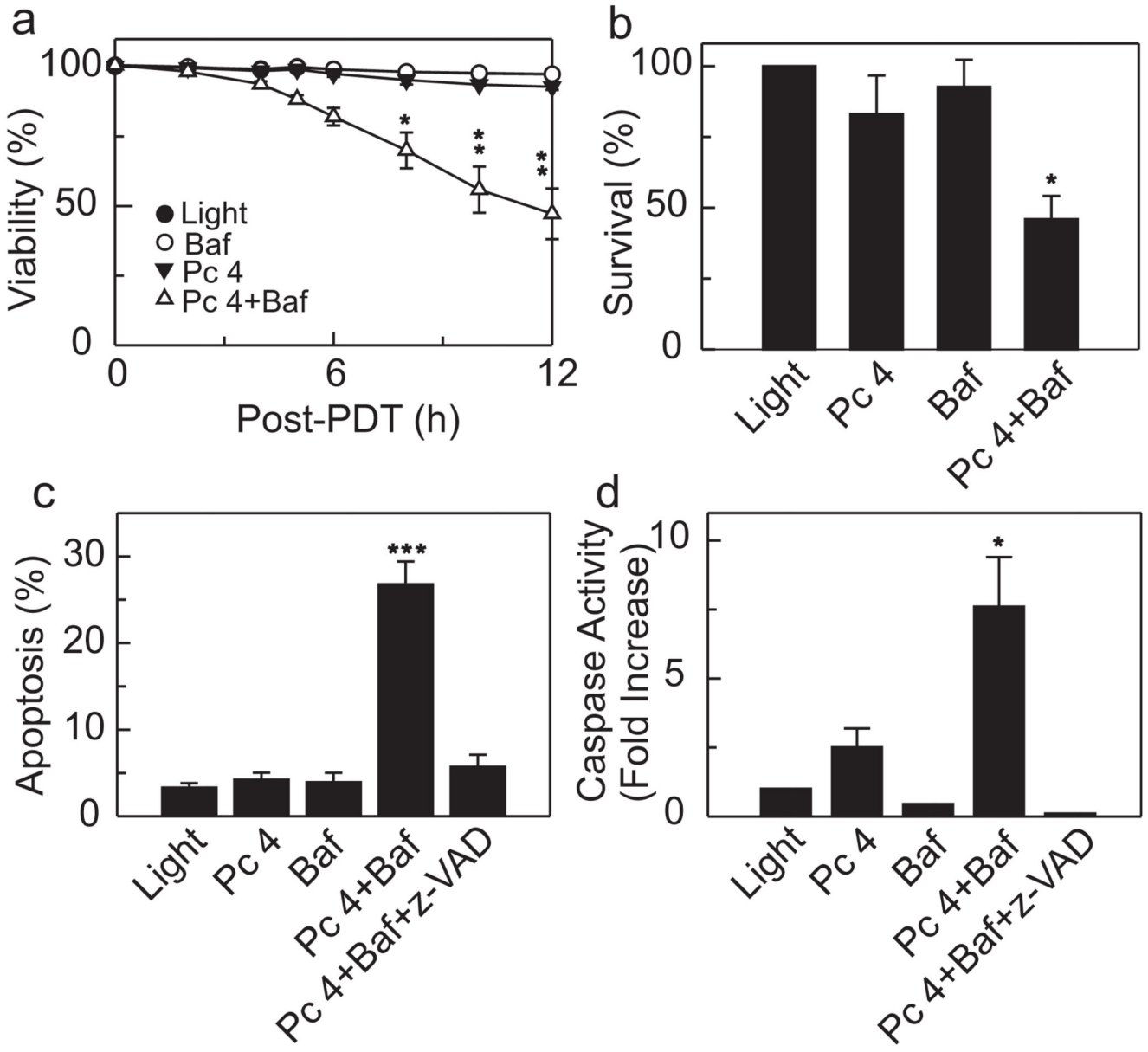

Figure 1.

Bafilomycin enhances Pc 4-PDT-mediated cell death. A431 cells were plated on 96-well plates (6 000 cells per well) and cultured for 24 h. Subsequently, cells were incubated with Pc 4 (25 nM) in FBS containing culture medium. After 18 h, medium was changed to fresh medium supplemented with Insulin-Transferrin-Selenium-X Reagent and PI (30 μM), but omitting FBS, followed by incubation with bafilomycin (50 nM; Baf) for 1 h, where indicated. Subsequently, cells were exposed to light as described in the Materials and Methods section. (a) Viability was assessed by PI exclusion using fluorometry. Results are expressed as percent viability at 0 h. Data represent three independent experiments (mean ± SEM) performed in quadruplicate. *$P < 0.05$; **$P < 0.01$ compared with Pc 4. (b) Cells (330 000 cells/6-cm Petri dish) were treated and irradiated as in (a). Subsequently, cells were

trypsinized and plated on 6-cm Petri dishes. After 14 days, colonies were stained with crystal violet and counted. Results are expressed as percent colonies of light-treated cultures. Data represent three or more independent experiments performed in triplicate. *$P < 0.05$ compared with Pc 4 (one-tailed *t*-test). (c) Cells were plated on 96-well plates (6 000 cells per well) and treated as described in (a). z-VAD (10 μ_M) was added, as indicated, 1 h prior to irradiation. Four hours after irradiation, apoptotic nuclei were scored with a fluorescence microscope as described in the Materials and Methods section. At least 200 cells were counted from three different microscopic fields for each treatment group. Results are expressed as percent apoptotic nuclei. Data represent three independent experiments (mean ± SEM) performed in triplicate. ***$P < 0.005$ compared with Pc 4. (d) Cells were plated on 6-well plates (120 000 cells per well) and treated as described in (a). Four hours after irradiation, cell lysates were prepared as described in the Materials and Methods section. Caspase 3/7 activity was normalized for protein content, and results are expressed as fold increase from light-treated cells. Data represent three independent experiments (mean ± SEM) performed in triplicate. *$P < 0.05$ compared with Pc 4 (one-tailed *t*-test).

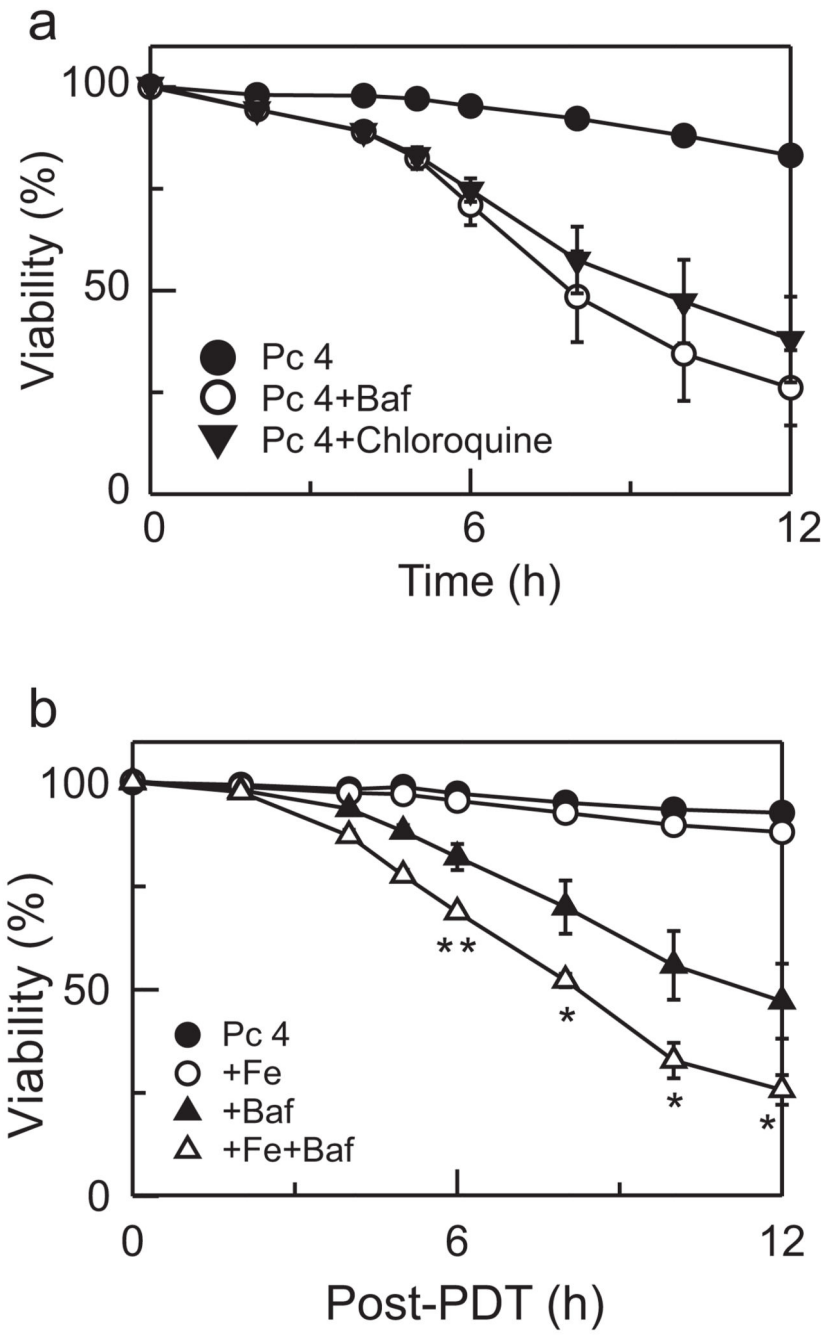

Figure 2.

Chloroquine enhances Pc 4-PDT-induced cell killing. (a) Cells were treated as described in Fig. 1a. As indicated, 50 nM bafilomycin or 50 μM chloroquine was added 1 h before irradiation, and cell viability was monitored with PI fluorometry. Results are expressed as percent viability of 0 h. Data represent three independent experiments performed in quadruplicate. (b) Cells were cultured in medium containing 30 μM Fe^{3+} for 24 h, as indicated. Subsequently, Fe^{3+} was washed out and cells were incubated with 25 nM Pc 4 for 18 h. Medium was replaced with medium supplemented with Insulin-Transferrin-Selenium-

X Reagent and omitting FBS. Bafilomycin was added, as indicated. Cell viability was monitored with PI fluorometry. Data represent three independent experiments (mean ± SEM) performed in quadruplicate. *$P < 0.05$; **$P < 0.01$ compared with Pc 4 + Baf.

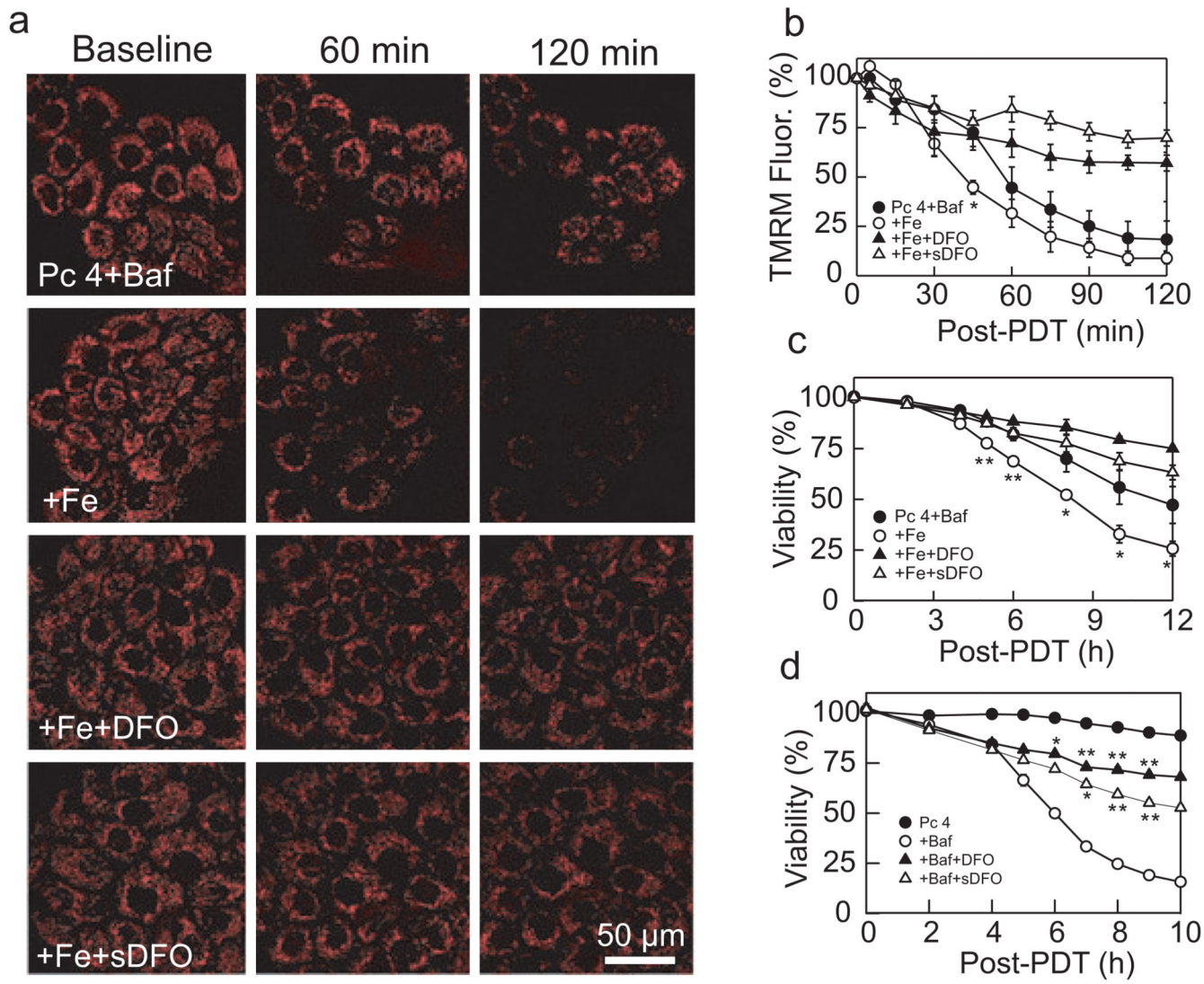

Figure 3.

Bafilomycin enhances Pc 4-PDT-mediated mitochondrial depolarization. (a) Cells were cultured on glass-bottomed Petri dishes in the presence and absence of Fe^{3+}(30 μM), as indicated. Subsequently, cells were incubated with Pc 4 (25 nM) in the presence and absence of DFO (1 mM) or sDFO for 18 h. Cells were loaded with 250 nM TMRM and subsequently incubated with TMRM (50 nM) and bafilomycin (Baf, 50 nM) for 1 h before irradiation. Red fluorescence of TMRM was imaged with laser scanning confocal microscopy before (0 min) and at 60 and 120 min after irradiation. Note loss of TMRM fluorescence after Pc 4-PDT in presence of Baf + Fe, which was prevented by DFO and sDFO. Representative images from three independent experiments. (b) average TMRM fluorescence after background subtraction under conditions described in panel (a) was determined every 15 min for 120 min. Results are expressed as percent TMRM fluorescence of 0 min. Data are means calculated from analyses of 82–100 cells per treatment group obtained from three independent experiments (mean ± SEM). *$P < 0.05$ compared with Pc 4 + Baf. (c) Cells were plated on 96-well plates and treated under same conditions as in panel (a). Viability

was monitored using PI fluorometry. Results are expressed as percent viability of 0 min. Data represent three independent experiments (mean ± SEM) performed in quadruplicate. **P* < 0.05; ***P* < 0.01 compared with Pc 4 + Baf. (d) Cells were exposed to Pc 4 (50 nM), Pc 4-PDT and Pc 4-PDT + Baf in the presence and absence of DFO and sDFO. **P* < 0.05; ***P* < 0.01 compared to Pc 4 + Baf.

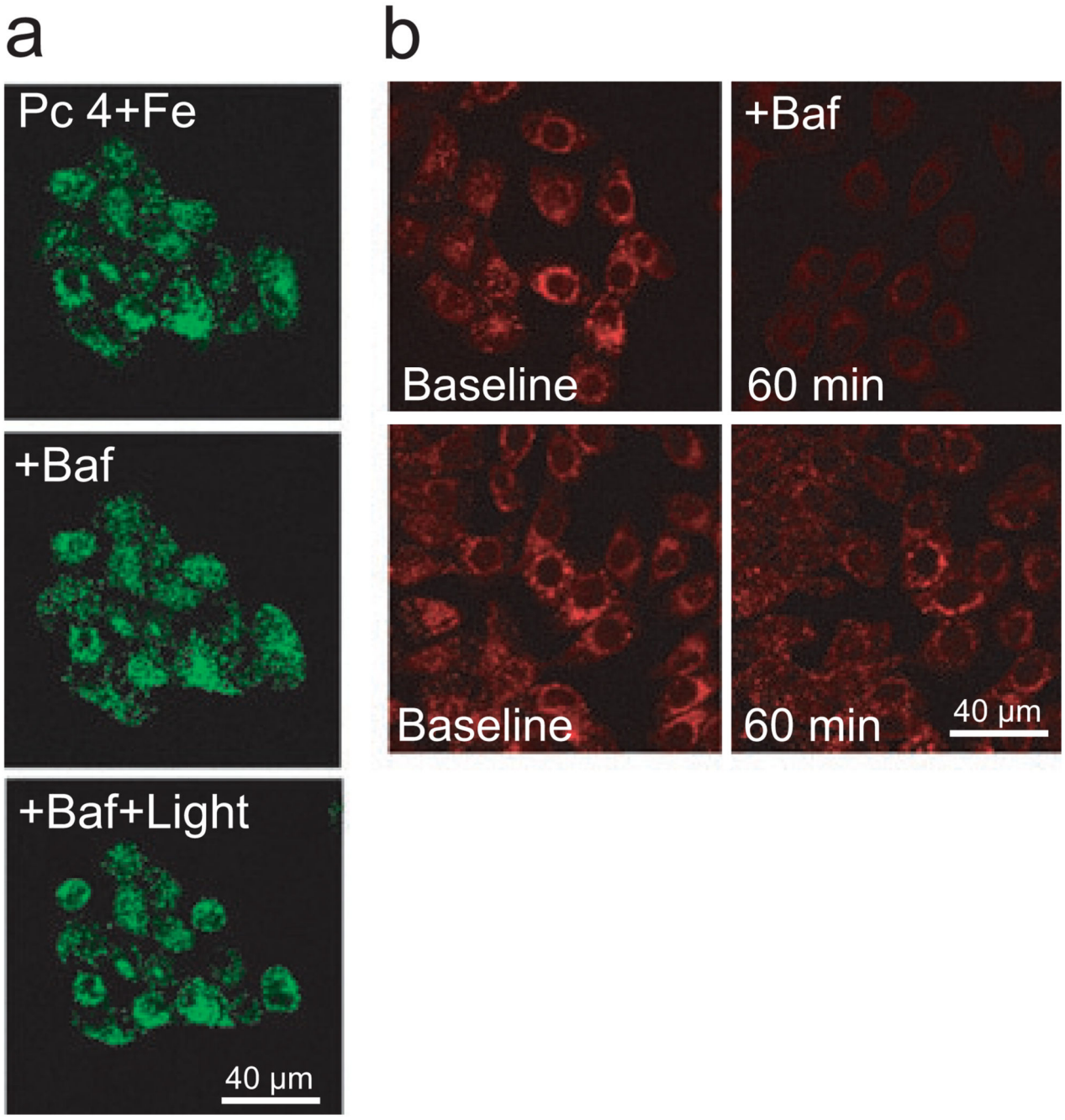

Figure 4.

Lysosomal membrane permeability after bafilomycin and Pc 4-PDT. (a) Cells were plated on glass-bottomed Petri dishes (150 000 cells per dish) in the presence of Fe^{3+}. After 24 h, medium was replaced with fresh medium containing 25 n_M Pc 4 and Alexa-488 dextran (10 kDa, 0.2 mg mL^{-1}). After 18 h, medium was replaced with fresh medium supplemented with ITX reagent and omitting FBS. Dishes were placed on a confocal microscope stage at 37°C. Images were obtained after Pc 4 and Fe^{3+} (Pc 4 + Fe), after 1 h exposure to bafilomycin (+ Baf) and after 2 h exposure to light (+ Baf + Light). (b) Cells were loaded

with LysoTracker Red (500 nM) for 20 min. Medium was replaced with fresh medium supplemented with 200 nM LysoTracker Red. After collecting a baseline image, bafilomycin (50 nM) was added and the images were taken after 60 min (upper panel). Lower panel shows untreated cells imaged before and after 60 min. Images (a and b) are representative of three independent experiments.

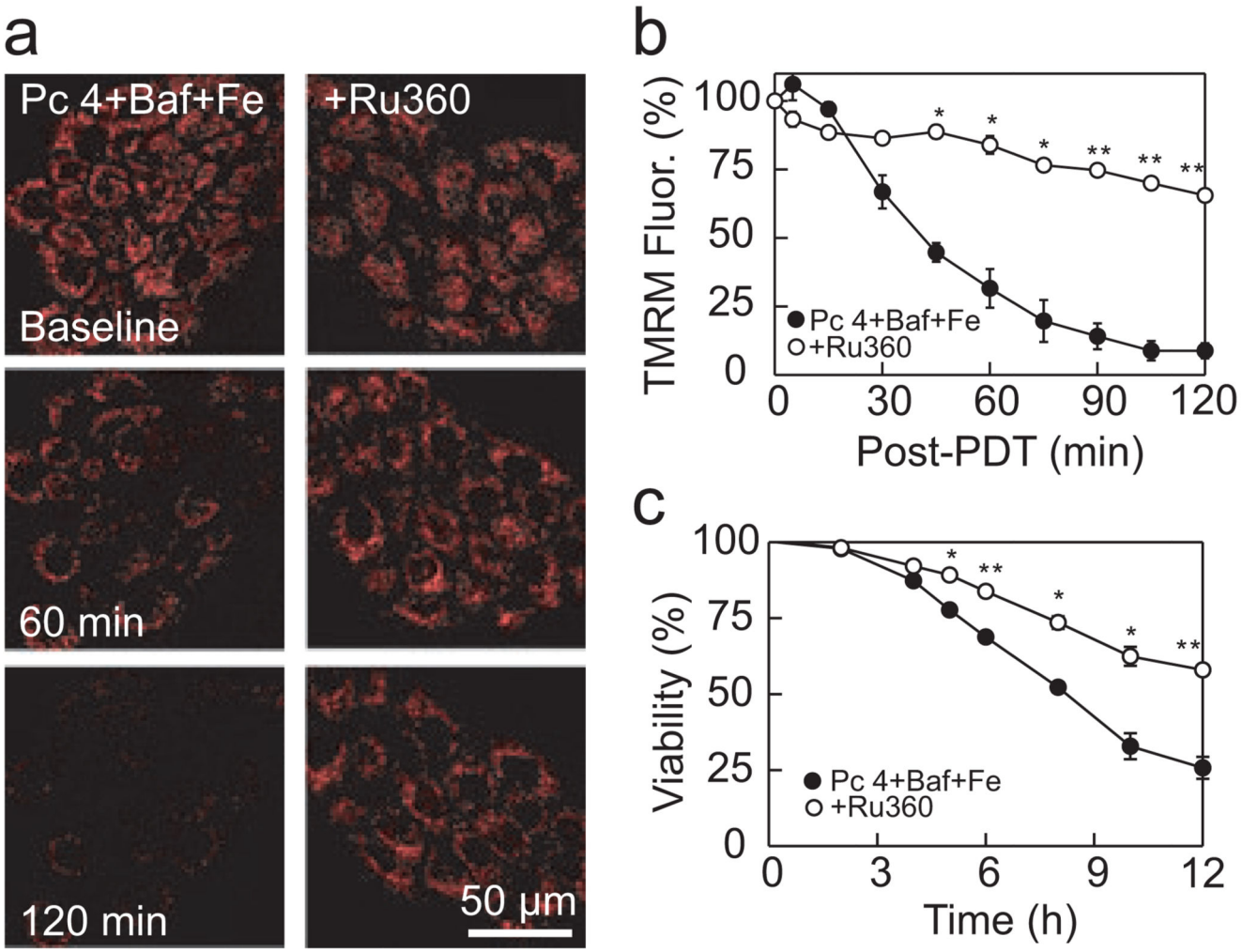

Figure 5.

Protection against mitochondrial depolarization by Ru360. (a) Cells were cultured in medium containing 30 μ_M Fe^{3+} for 24 h, as indicated. Then, Fe^{3+} was washed out and cells were incubated with Pc 4 (25 n_M) and Ru360 (10 μ_M) for 18 h. Subsequently, cells were loaded with TMRM and incubated with bafilomycin (50 n_M) for 1 h before irradiation, as described in Fig. 4a. TMRM fluorescence was imaged with confocal microscopy as described in the Materials and Methods section. Ru360 prevented the loss of TMRM fluorescence after Pc 4-PDT with Baf + Fe. Representative images from four independent experiments are shown. (b) Average TMRM fluorescence was quantified for the experiments described in panel (a). Data are means calculated from analyses of 82–125 cells per treatment group obtained from three to four experiments (means ± SEM). (c) Cell viability was monitored using PI fluorometry under same conditions as panel (a) from three independent experiments performed in quadruplicate. *P < 0.01; **P < 0.001 compared with Pc 4 + Baf + Fe.

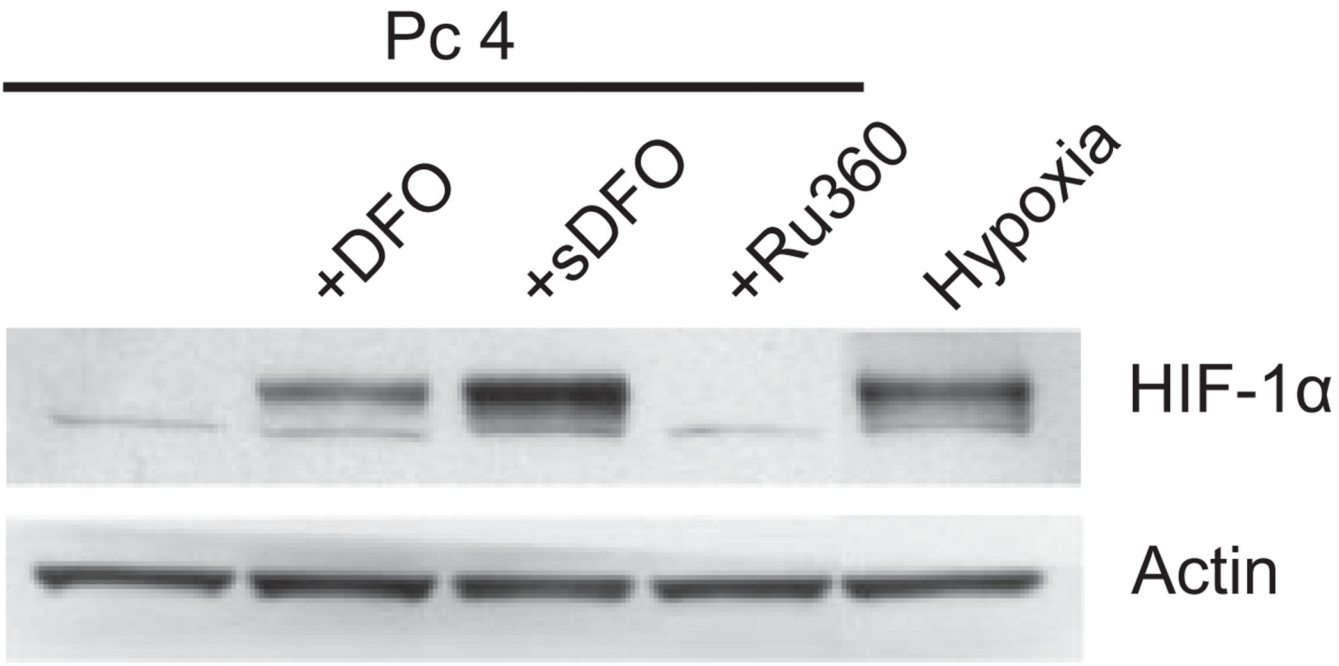

Figure 6.

Effect of iron chelators and Ru360 on HIF-1α protein levels. Cells were incubated with Pc 4 (25 nM) in the presence and absence of DFO (1 mM), sDFO (1 mM) and Ru360 (10 μM) for 18 h, and cell lysates were subjected to Western blotting. Cells were also exposed to hypoxia (0.5% O_2) for 6 h as a positive control. Actin was used as a loading control. Blots are representative of three independent lysates.

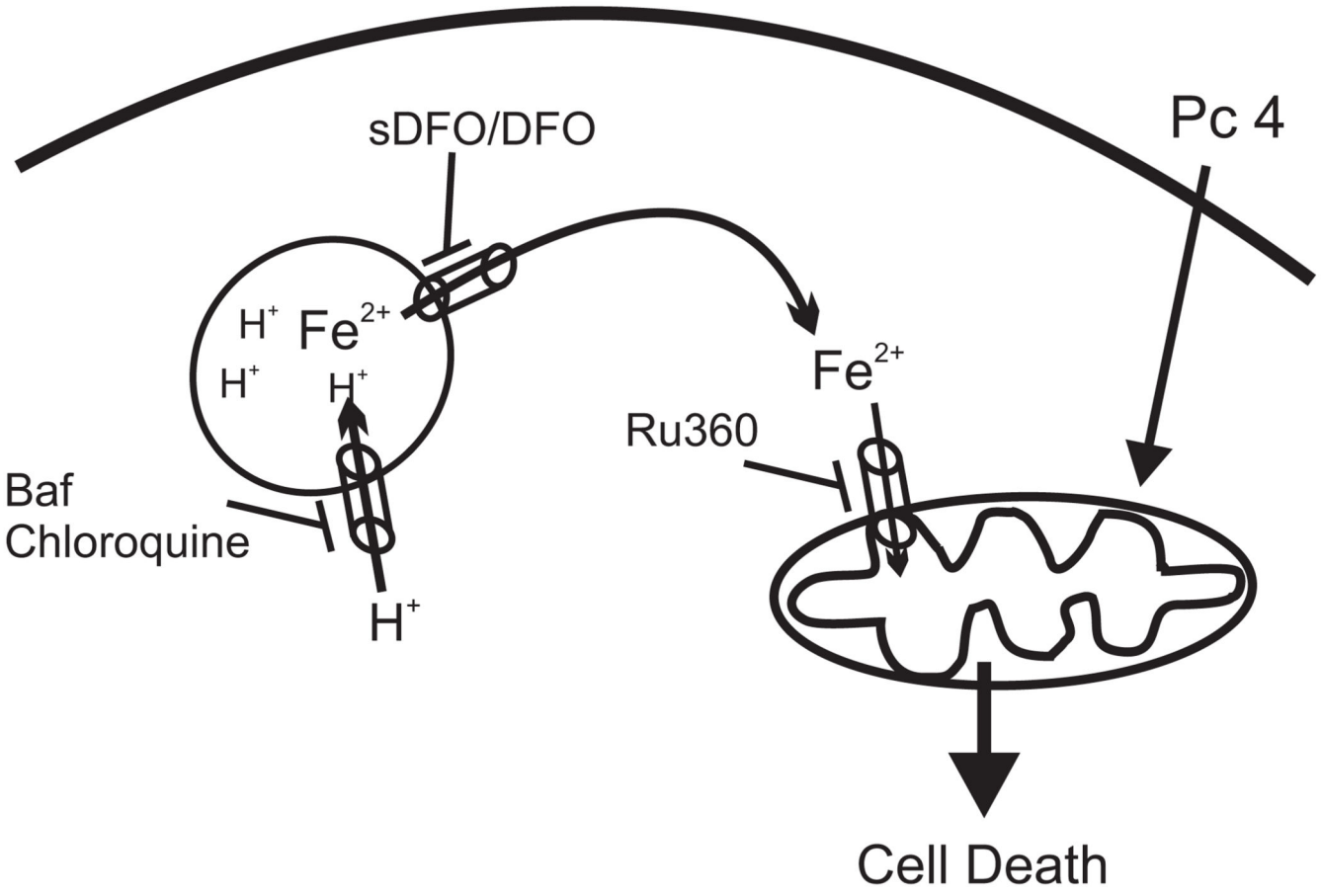

Figure 7.
Proposed model for interplay between lysosomes and mitochondria during PDT.